Zinc-dysprosium functionalized amyloid fibrils

Article (Accepted Version)

Journal Name

COMMUNICATION

Zinc-Dysprosium functionalized amyloid fibrils

Stavroula I. Sampani,[a] Youssra K. Al-Hilaly,[a,b] Sharali Malik,[c] Louise C. Serpell*[a] and George E. Kostakis*[a]

Received 00th January 20xx,
Accepted 00th January 20xx

DOI: 10.1039/x0xx00000x

www.rsc.org/

The heterometallic Zn_2Dy_2 entity bearing partially saturated metal centres covalently decorates a highly ordered amyloid fibril core and the functionalised assembly exhibits catalytic Lewis acid behaviour.

Amyloid fibrils represent a class of self-assembled peptides that share a very well ordered, cross-β core structure and are suitable for further decoration.[1] Although amyloid is well known for a pathological role in diseases such as Alzheimer's disease and Diabetes type 2, short self-assembling peptides have been developed and characterised as templates for functionalisation.[2–4] Hexapeptides have been particularly useful in forming highly ordered amyloid cores and several of these have been characterised to provide structural information. X-ray fibre diffraction, transmission electron microscopy have been combined to provide a cross-β structural model for the self-assembling peptide sequence HIS-TYR-PHE-ASN-ILE-PHE (HYFNIF),[5] HYFNIF along with several other hexapeptides was first identified as a highly amyloidogenic peptide sequence using the amyloid propensity algorithm WALTZ.[6] This amyloid-forming peptide contains several side chains that are ideal for further functionalisation. Peptides containing histidine residues are the most widely studied in coordination chemistry, due to their presence in many important metalloproteins.[7]

Functionalisation of these entities with metals depends on several parameters, i.e. lability of metal centres, use of protic solvents, and the presence of other amino acids with specific coordinating side chains, such as Asn, Glu and Met.[8,9] Recently, the successful self-assembly of biomolecules and metal centres has yielded various supramolecular architectures[10] i.e. macrocycles, cages, metal-organic frameworks,[11–15] spherical shells or fibrils,[16,17] of which some exhibit biomimetic functions such as selective recognition[18] and allosteric cooperativity.[19]

In protic solvents, we have established the structural integrity and the transformative character, of the bimetallic entity $[Zn^{II}_2Dy^{III}_2L_4(NO_3)_2(DMF)_2]$ (**Zn_2Dy_2**) (Figure 1, left).[20,21] The **Zn_2Dy_2** entity is centrosymmetric and can be considered as an ideal moiety to bind with histidine containing biomolecules because is a) built solely by the organic ligands which partially saturate the coordination environment of all metal centres (the remaining sites are occupied by exchangeable solvent and anion molecules) and b) the metal centres in the **Zn_2Dy_2** unit are in a close proximity (3.3Å); Dy is oxophilic and Zn can coordinate to N-atoms, thus permitting either the Zn (A), or Dy (B) or both (A&B) centres to bind to one or two positions in the biomolecule (Figure 1, left). We utilised capped-HYFNIF (Figure 1, right) as model peptide to investigate its binding to **Zn_2Dy_2**, as it contains various binding sites, starting with the histidine in position-1 as well as one tyrosine residue in position-2 with the -OH group of the phenolic ring. Here we have fully characterised the complexation and architecture of the functionalised amyloid structure.

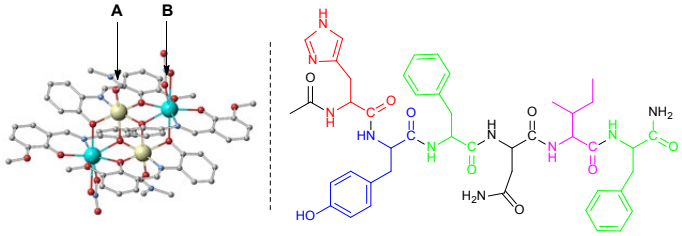

Figure 1. (left) A structure of the **Zn_2Dy_2** entity used for binding; **A** and **B** point potential binding sites . (right) A ChemDraw representation of the capped-HYFNIF molecule used in this study.

HYFNIF self-assembles to form amyloid-like fibrils, which are characterised by their regular cross-β architecture.[5] Capped HYFNIF (2mg/ml) forms mature fibrils in H_2O after 7 days incubation (Figure 2B). CD spectra for HYFNIF in water revealed a strong, positive signal at 200 nm which indicates a linear dichroism (LD) contribution arising from the alignment of the fibrils and this has been previously reported for HYFNIF fibrils.[5]

[a]*School of Life Sciences, University of Sussex, Falmer, BN1 9QG, United Kingdom E-mail: L.c.serpell@sussex.ac.uk, G.Kostakis@sussex.ac.uk,*
[b]*Chemistry Department, College of Science, Mustansiriyah University, Baghdad, Iraq*
[c]*Institute of Nanotechnology, Karlsruhe Institute of Technology (KIT), Hermann-von-Helmholtz-Platz 1, 76344 Eggenstein-Leopoldshafen, Germany*

† Electronic Supplementary Information (ESI) available: See DOI: 10.1039/x0xx00000x

CD spectra recorded at 0° and 90° confirmed LD arising from lateral alignment of the fibrils. CD showed a small signal at 275 nm (inset, Figure 2A) attributed to the tyrosine residue.

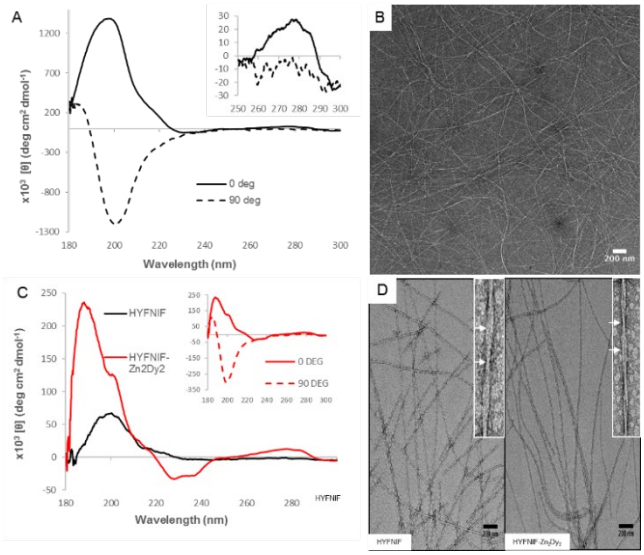

Figure 2. (A) The CD spectra of 2.4 x10^{-3} M HYFNIF in water at 0° and 90°. The signal at 275 nm (CD spectra) is attributed to tyrosine residue. (B) Transmission electron microscopy images of HYFNIF amyloid fibres in water. (C) CD spectra of HYFNIF untreated (black) and treated with Zn_2Dy_2 (red), in H_2O-MeOH and incubated for 24 h at room temperature. (inset) CD spectrum of **HYFNIF-Zn_2Dy_2** was collected at 0° and 90°. (D) Transmission electron microscopy images of HYFNIF amyloid-like fibres in H_2O-MeOH without and with **Zn_2Dy_2**.

HYFNIF amyloid-like fibrils were incubated with **Zn_2Dy_2** for 24 h in aqueous methanol at room temperature and any conformational changes were monitored using CD and compared to the CD spectrum of HYFNIF in aqueous methanol alone (Figure 2C). The CD spectra of HYFNIF in water and methanol are similar (black traces, Figure 2A, 2C). However, the CD spectrum of **Zn_2Dy_2**-treated HYFNIF fibrils in aqueous methanol shows the appearance of new signals at 190, 202, 230, and 238 nm with significantly enhanced contribution from the tyrosine residue at 275 nm as well as an increased intensity at 202 nm. This enhanced signal indicates changes in the vicinity of the tyrosine residue which may suggest the binding of the tyrosine residue with the **Zn_2Dy_2** entity. The signal at 202 nm belongs to LD contribution as shown by the CD spectra that were collected at 0 and 90 deg (inset, Figure 2C). To investigate the effect of the **Zn_2Dy_2** entity on the HYFNIF fibrils, 1.26x10^{-3} M HYFNIF fibrils in aqueous methanol were treated with metal sources **Zn_2Dy_2** (**HYFNIF-Zn_2Dy_2**), $Zn(NO_3)_2.6H_2O$ (HYFNIF-Zn), $Dy(NO_3)_3.5H_2O$ (HYFNIF-Dy) or $Zn(NO_3)_2.6H_2O/Dy(NO_3)_3.5H_2O$ (HYFNIF-Zn-Dy) and incubated for 24 h at room temperature. The CD spectra with Zn, Dy or Zn-Dy alone did not appear to show contribution of LD and gave a signal at 218nm consistent with β-sheet content and differed significantly from the spectrum arising from **HYFNIF-Zn_2Dy_2**. (Figure S1).

Transmission electron microscopy studies were performed to compare the morphology of HYFNIF in aqueous methanol and **HYFNIF-Zn_2Dy_2** in aqueous methanol (Figure 2D). These show the appearance of very thin fibrils in dense networks after one-week incubation, in all cases. HYFNIF in aqueous methanol forms ordered fibrils with dimensions of 8.85±0.73 nm STDEV short width, 12.69±1.62 nm STDEV long width, and 59.78±8.35 nm STDEV periodicity compared to **HYFNIF-Zn_2Dy_2** in aqueous methanol with dimensions of 9.38±0.57 nm STDEV short width, 11.99±1.24 nm STDEV long width, and 65.39±12.15 nm STDEV periodicity (Figure 2D). Therefore we can conclude that no significant morphological difference was observed after treating the preformed HYFNIF fibre with **Zn_2Dy_2**.

X-ray fibre diffraction (XRFD) confirms that the binding of **Zn_2Dy_2** to HYFNIF fibrils does not affect the core architecture. X-ray fibre diffraction patterns were collected for HYFNIF and **HYFNIF-Zn_2Dy_2** (Figure 3) showing the characteristic 4.7Å reflection on the meridian, arising from the hydrogen-bonded β-strands that run perpendicular to the fibre axis and 12 Å signal on the equator, arising from the spacing between the β-sheets. HYFNIF and the **HYFNIF-Zn_2Dy_2** fibres showed the lower angle reflections on the equator at 16 Å and 18 Å respectively, possibly suggesting that packing is affected by the introduction of the compound (Figure 3).

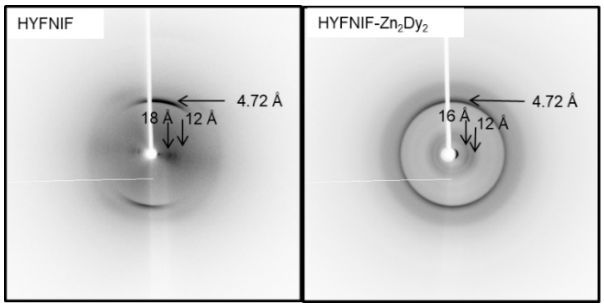

Figure 3. X-ray Fibre diffraction (XFRD) confirms that the decoration of the fibrils by Zn_2Dy_2 does not affect the structure of the core of the amyloid fibrils.

UV-Vis data were recorded in the region of 190-800 nm. Zn^{II} is diamagnetic ($3d^{10}$), whilst Dy has a $4f^9$ electronic configuration, thus all transitions are very weak and the observed peaks are anticipated to correspond to metal-to-ligand charge transfer (MLCT) bands. Indeed, the UV-Vis spectrum of **Zn_2Dy_2** shows a peak in the 400-460 nm region which may be attributed to a MLCT band (Figure 4), however this peak is shifted by 100nm, at 350 nm, in the **HYFNIF-Zn_2Dy_2** spectrum (Figure 4, inset). In the UV region, in agreement with the CD data, the **HYFNIF-Zn_2Dy_2** exhibits a maximum (at 275 nm) with significant signal enhancement comparing to the maximum exhibited by the HYFNIF. Notably, the **Zn_2Dy_2** entity does not show any peak at this area. This peak can be attributed to the presence of aromatic tyrosine residues in the fibril (Figure 4, red and black lines).[5] These findings support the successful binding of the **Zn_2Dy_2** entity to HYFNIF. Within the region 300-500 nm, the presence of two minima at 308 and 401 nm and one maximum at 347 nm in the **HYFNIF-Zn_2Dy_2** spectrum, comparing to the three maxima at 308, 378, 417 nm and a minimum at 343 nm of the **Zn_2Dy_2** unit further indicates binding of the peptide to the metals of the coordination cluster (inset, Figure 4). Strong absorption appeared near 200-240 nm for the HYFNIF, while in the same region, Zn-Dy and Dy salts slightly induced hypochromicity in the peptide solutions (Figure 4 and Figure S3). Previous studies have indicated the spatial structure

together with the chirality of the chromophores (C=O,–COOH) and auxochromes (–OH, –NH_2) of peptides change upon zinc binding,[22,23] inducing changes in the absorption intensity. According to the literature, lanthanides have been found to accelerate fibrillation,[24] while zinc can inhibit fibril formation[25] and promote intermolecular interactions[26] or indirectly inhibit/change the binding mode of other metals.[27] The latter may also occur here, where zinc salt and dysprosium salt co-exist with HYFNIF (HYFNIF-Zn-Dy). Moreover, bearing in mind that Tyr-10 fluorescence is a better tracker for interactions with amyloids,[28,29] we recorded a set of data (Figure S3). After 24h of incubation for HYFNIF and treated HYFNIF, in the area 300-320 nm, where the characteristic Tyrosine fluorescent emission is observed, we identify that HYFNIF exhibits a maximum with intensity 345, HYFNIF-metal salts (Zn and Dy) exhibits a maximum with intensity 305, whilst the **HYFNIF-Zn_2Dy_2** exhibits a maximum with intensity 132. The suppression of the tyrosine signal of **HYFNIF-Zn_2Dy_2** may indicate that **Zn_2Dy_2** binds to the Tyrosine. When salts of both metals were incubated with HYFNIF, a significant difference in interaction is observed; this may signifies the antagonistic behaviour of both metal centres for binding or the inhibition of the fibril formation.

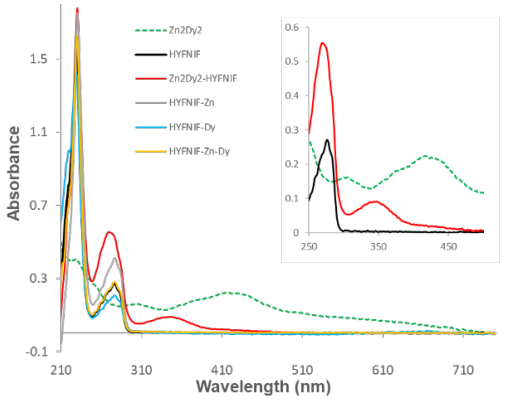

Figure 4. UV-Vis spectra of the **Zn_2Dy_2** entity and HYFNIF fibrils treated and untreated with Zn/Dy sources in H_2O-MeOH, incubated for 24 h at room temperature. (inset) The absorption minima at at 308 and 401 nm, the enhanced maximum at 275 and the maximum at 347 nm in the HYFNIF-Zn_2Dy_2 spectrum support binding of the coordination cluster to the peptide.

To further identify the elemental composition of the functionalised **HYFNIF-Zn_2Dy_2** entity field emission scanning electron microscope studies with energy dispersive X-ray spectroscopy (FESEM/EDX) were recorded despite their qualitative rather than quantitative character. **HYFNIF-Zn_2Dy_2**, suspended in Milli-Q H_2O-MeOH, was prepared by pipetting a drop onto a polished Si chip and dried overnight at room temperature to afford a light yellow film. The measurements are summarized in Table S2 and demonstrate the presence of Zn, Dy, O, C and N elements and that a 1:1 Zn:Dy ratio is reasonable.

Furfural and amines yield, via a Lewis acid promoted domino reaction, *trans*-4,5-diaminocyclopent-2-enones (Table 1); this synthon is a versatile building block in the synthesis of natural products and therefore several methodologies that promote this reaction have been developed.[30–32] In previous work, we developed a bimetallic catalyst that efficiently catalysed this transformation.[31] To identify the catalytic efficacy of the functionalised **HYFNIF-Zn_2Dy_2**, several screening experiments were performed (Table 1, Entries 1-8). The catalytic conversion was performed in a 10^{-3} M scale and we used environmental friendly solvents. From these data, it is evident that the reaction is promoted by the metal salts under the present protocol in a moderate yield. Then, we tested HYFNIF (Table 1, entry 5), as well as combinations of HYFNIF with metal salts (Table 1, entries 6 – 8). The HYFNIF fibril is not catalytically active, but the small conversion may be attributed to the solvent, as this has been noted by others[32] and our initial experiments (Table 1, entry 1). The moderate catalytic performance of the *in-situ* generated HYFNIF-metal salts derivatives (Table 1, entries 6 – 8) and the almost identical yields when compared with that of the metal salts (Table 1, Entry 4) indicates that the metal salts are responsible for the conversion. Then, we tested the tetranuclear **Zn_2Dy_2** unit under similar conditions (Table 1, entry 9), which exhibited very good catalytic behaviour. The functionalised **HYFNIF-Zn_2Dy_2** moiety promotes the transformation slightly better, when compared with metal salts (Table 1, Entry 4) and in situ mixtures (Table 1, Entries 6-8) and with full completion after four days (Table 1, entry 10). To further validate the potential catalytic efficacy of **HYFNIF-Zn_2Dy_2** we employed a primary amine, aniline, (Table 1, entry 11), and the entity was found to be catalytically active with a very good yield of product. Notably, simple metal salts such as $Cu(OTf)_2$ or $Dy(OTf)_3$ fail to promote this transformation.[33,34] It is worth noting that the major product of this reaction is the open derivative (Stenhouse salt) as we have noted previously, which upon acidic treatment yields the closed ring derivative.[31] The present data identify the applicability of the present catalytic protocol, i.e mixture of non-protic/protic solvents, concentration (10^{-3} M) and that **HYFNIF-Zn_2Dy_2** is a promising Lewis acid candidate that may be used in future studies at a nanoscale level.

Table 1. The catalysed formation of *trans*-4,5-diaminocyclopen-2-enone[a].

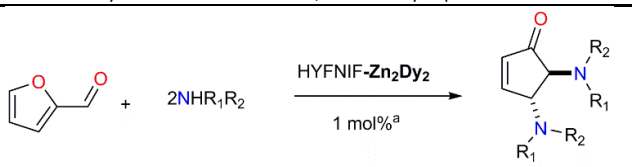

Entry	Catalyst	Solvent[b]	Amine	Yield%[c]
1	-	A	Morpholine	2
2	-	B	Morpholine	8
3	-	C	Morpholine	8
4	$Zn(NO_3)_2.6(H_2O)$ + $Dy(NO_3)_3.5(H_2O)$	C	Morpholine	53
5	HYFNIF	C	Morpholine	2 (3[d])
6	HYFNIF + $Zn(NO_3)_2.6(H_2O)$	C	Morpholine	56
7	HYFNIF + $Dy(NO_3)_3.5(H_2O)$	C	Morpholine	57
8	HYFNIF + $Zn(NO_3)_2.6(H_2O)$ + $Dy(NO_3)_3.5(H_2O)$	C	Morpholine	58

9	**Zn_2Dy_2**	C	Morpholine	95
10	**HYFNIF-Zn_2Dy_2**	C	Morpholine	67(100[d])
11	**HYFNIF-Zn_2Dy_2**	C	Aniline	84(100[d])

[a] Room Temperature, concentration 3mM, 1% Catalyst loading, using the working peptide solutions of $1.26x10^{-3}$ mol/L in HYFNIF, Total volume (0.25mL), Time 24h, Ambient conditions. [b]Solvent: A = MeOH, B = MeCN, C = MeCN/MeOH (4/1). [c]Calculated by ^{1}H-NMR, based on the conversion of furfural. [d] After 96 hours.

Protic solvents are strong coordinating ligands, which may occupy the coordination sites of the metal centres or favour metal hydrolysis, leading to unsuccessful binding or quench of the desired property. Moreover, terminally acetylated peptides containing histidine tend to form imidazole coordinated complexes with transition metals in slightly acidic or neutral solutions. However, for Zn(II), hydrolysis can mainly be observed in basic solutions.[35] Ln centres are oxophilic and therefore can bind to O atoms, such as the OH group of the tyrosine moiety of HYFNIF. Bearing all these in mind, we propose a binding model of HYFNIF through the N atom of His (Zn) and possibly through the neighbouring –OH group of Tyr (Dy), shown in Figure 5 and possible coordination mode(s) of the ligand (Fig S4).

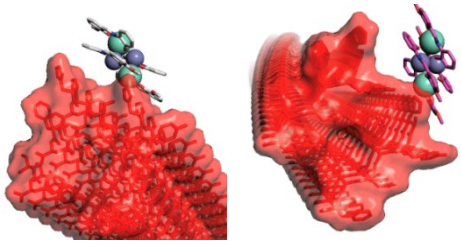

Figure 5. Proposed model of the **HYFNIF-Zn_2Dy_2** fibrils.

In summary, the present study demonstrates the successful implementation of a well-known **Zn_2Dy_2** molecular robust entity in decorating an amyloid HYFNIF core. Despite the significant flexibility the **Zn_2Dy_2** moiety possesses and the use of protic solvent for the assembly, a successful binding to HYFNIF fibril is observed. Furthermore, despite harsh solvents used, the HYFNIF fibril architecture remains stable and unchanged as a core template. The success of the proposed methodology is attributed to the limited coordination sites in the **Zn_2Dy_2** entity available for coordination with HYFNIF and the presence of histidine groups (N-donor atoms), thus paving the way for future development. A range of techniques have been used to validate this notion. Interestingly, the resulting functionalized entity **HYFNIF-Zn_2Dy_2** was found to promote the Lewis acidic transformation of furfural and amines to yield the corresponding cyclopentenones. These very promising results open new avenues for several research fields including Coordination Chemistry, Biochemistry and Catalysis.

GEK acknowledges the EPSRC (UK) for funding (grant number EP/ M023834/1). YKA acknowledges Mustansiriyah University, Baghdad, Iraq (www.uomustansiriyah.edu.iq) for support. SM acknowledges support by the Helmholtz society through program Science and Technology of Nanosystems (STN). The authors would like to thank Dr Pascale Schellenberger for help with transmission electron microscopy and networking support by the COST Action MultiComp (CA15107), supported the COST Association (European Cooperation in Science and Technology).

Notes and references

1 S. L. Gras, in *Advances in Chemical Engineering*, Academic Press, 2009, vol. 35, pp. 161–209.
2 Z. S. Al-Garawi, K. L. Morris, K. E. Marshall, J. Eichler and L. C. Serpell, *Interface Focus*, 2017, **7**, 20170027.
3 J. Madine, H. A. Davies, C. Shaw, I. W. Hamley and D. A. Middleton, *Chem. Commun.*, 2012, **48**, 2976–2978.
4 Z. S. Al-Garawi, B. A. McIntosh, D. Neill-Hall, A. A. Hatimy, S. M. Sweet, M. C. Bagley and L. C. Serpell, *Nanoscale*, 2017, **9**, 10773–10783.
5 K. L. Morris, A. Rodger, M. R. Hicks, M. Debulpaep, J. Schymkowitz, F. Rousseau and L. C. Serpell, *Biochem. J.*, 2013, **450**, 275–283.
6 S. Maurer-Stroh, M. Debulpaep, N. Kuemmerer, M. L. De La Paz, I. C. Martins, J. Reumers, K. L. Morris, A. Copland, L. Serpell, L. Serrano, J. W. H. Schymkowitz and F. Rousseau, *Nat. Methods*, 2010, **7**, 237–242.
7 M. Laitaoja, J. Valjakka and J. Jänis, *Inorg. Chem.*, 2013, **52**, 10983–10991.
8 H. Kozl, W. Bal, M. Dyba and T. Kowalik-Jankowska, *Coord. Chem. Rev.*, 1999, **184**, 319–346.
9 I. Sóvágó, E. Farkas and A. Gergely, *J. Chem. Soc. Dalt. Trans.*, 1982, 2159–2163.
10 T. Sawada, A. Matsumoto and M. Fujita, *Angew. Chemie Int. Ed.*, 2014, **53**, 7228–7232.
11 T. R. Cook and P. J. Stang, *Chem. Rev.*, 2015, **115**, 7001–7045.
12 B. M. Schmidt, T. Osuga, T. Sawada, M. Hoshino and M. Fujita, *Angew. Chemie Int. Ed.*, 2016, **55**, 1561–1564.
13 W. Wang, Y.-X. Wang and H.-B. Yang, *Chem. Soc. Rev.*, 2016, **45**, 2656–2693.
14 L. J. Chen, Y. Y. Ren, N. W. Wu, B. Sun, J. Q. Ma, L. Zhang, H. Tan, M. Liu, X. Li and H. B. Yang, *J. Am. Chem. Soc.*, 2015, **137**, 11725–11735.
15 L. J. Chen and H. B. Yang, *Acc. Chem. Res.*, 2018, **51**, 2699–2710.
16 S. Burazerovic, J. Gradinaru, J. Pierron and T. R. Ward, *Angew. Chemie Int. Ed.*, 2007, **46**, 5510–5514.
17 J. D. Brodin, X. I. Ambroggio, C. Tang, K. N. Parent, T. S. Baker and F. A. Tezcan, *Nat. Chem.*, 2012, **4**, 375–382.
18 M. Baskin and G. Maayan, *Chem. Sci.*, 2016, **7**, 2809–2820.
19 J. P. Miller, M. S. Melicher and A. Schepartz, *J. Am. Chem. Soc.*, 2014, **136**, 14726–9.
20 K. Griffiths, P. Kumar, G. R. Akien, N. F. Chilton, A. Abdul-Sada, G. J. Tizzard, S. J. Coles and G. E. Kostakis, *Chem. Commun.*, 2016, **52**, 7866–7869.
21 K. Griffiths, A. C. Tsipis, P. Kumar, O. P. E. Townrow, A. Abdul-Sada, G. R. Akien, A. Baldansuren, A. C. Spivey and G. E. Kostakis, *Inorg. Chem.*, 2017, **56**, 9563–9573.
22 A. Armas, V. Sonois, E. Mothes, H. Mazarguil and P. Faller, *J. Inorg. Biochem.*, 2006, **100**, 1672–1678.
23 R. P. Houser, M. P. Fitzsimons and J. K. Barton, *Inorg. Chem.*, 1999, **38**, 1368–1370.
24 J. Bai, Z. Zhang, M. Liu and C. Li, *BMC Biophys.*, 2016, **9**, 1–10.
25 O. V. Bocharova, L. Breydo, V. V. Salnikov and I. V. Baskakov,

Biochemistry, 2005, **44**, 6776–6787.
26 A. G. Kenward, L. J. Bartolotti and C. S. Burns, *Biochemistry*, 2007, **46**, 4261–4271.
27 E. D. Walter, D. J. Stevens, M. P. Visconte and G. L. Millhauser, *J. Am. Chem. Soc*, 2007, **129**, 15440–15441.
28 O. J. Rolinski, M. Amaro and D. J. S. Birch, *Biosens. Bioelectron.*, 2010, **25**, 2249–2252.
29 A. Khan, A. E. Ashcroft, O. V. Korchazhkina and C. Exley, *J. Inorg. Biochem.*, 2004, **98**, 2006–2010.
30 R. F. A. Gomes, J. A. S. Coelho and C. A. M. Afonso, *Chem. - A Eur. J.*, 2018, **24**, 9170–9186.
31 K. Griffiths, P. Kumar, J. D. Mattock, A. Abdul-Sada, M. B. Pitak, S. J. Coles, O. Navarro, A. Vargas and G. E. Kostakis, *Inorg. Chem.*, 2016, **55**, 6988–6994.
32 M. Nardi, P. Costanzo, A. De Nino, M. L. Di Gioia, F. Olivito, G. Sindona and A. Procopio, *Green Chem.*, 2017, **19**, 5403–5411.
33 S.-W. Li and R. A. Batey, *Chem. Commun.*, 2007, 3759–3761.
34 R. F. A. Gomes, N. R. Esteves, J. A. S. Coelho and C. A. M. Afonso, *J. Org. Chem.*, 2018, **83**, 7509–7513.
35 I. Sóvágó, K. Várnagy, N. Lihi and Á. Grenács, *Coord. Chem. Rev.*, 2016, **327–328**, 43–54.